# Electronic Supplementary Information

## Distance-triggered signaling on-off mechanism by plasmonic Au nanoparticles: toward advanced photocathodic DNA bioanalysis

Gao-Chao Fan[a], Huan Zhao[a], Linzheng Ma[ab], Yanwei Lu[a] and Xiliang Luo*[a]

[a] Key Laboratory of Optic-electric Sensing and Analytical Chemistry for Life Science, MOE; Shandong Key Laboratory of Biochemical Analysis; College of Chemistry and Molecular Engineering, Qingdao University of Science and Technology, Qingdao 266042, China

[b] College of Chemical and Environmental Engineering, Shandong University of Science and Technology, Qingdao 266590, China

*E-mail: xiliangluo@qust.edu.cn

## Section 1: Experimental

**Materials and Reagents.** Hexamethylenetetramine ($C_6H_{12}N_4$) and nickel (II) nitrate hexahydrate ($NiNO_3 \cdot 6H_2O$) were purchased from Shanghai Titan Scientific Co., Ltd. (China). Cadmium chloride ($CdCl_2 \cdot 2.5H_2O$), sodium tellurite ($Na_2TeO_3$), chloroauric acid ($HAuCl_4 \cdot 4H_2O$), sodium hydroxide (NaOH), and sodium chloride (NaCl) were ordered from Aladdin Reagent Inc. (China). Trisodium citrate dehydrate and sodium borohydride ($NaBH_4$) were purchased from Sinopharm Chemical Reagent Co., Ltd (China). N-hydroxysuccinimide (NHS), 1-ethyl-3-(3-dimethylaminopropyl) carbodiimide hydrochloride (EDC), monoethanolamine (MEA), poly(diallyldimethylammonium chloride) (PDDA), 3-mercaptopropionic acid (MPA), and 6-mercaptohexanol (MCH) were ordered from Sigma-Aldrich (USA). ITO electrodes (type JH52, ITO coating 30±5 nm, sheet resistance ≤ 10 Ω/square) were obtained from Beijing Zhongjingkeyi Technology Co., Ltd. (China). All aqueous solutions were prepared by deionized water (DI water, 18 MΩ/cm) from a Milli-Q water purification system. The DNA solution, washing buffer solution, and blocking buffer solution (containing 1 mM MEA) were all prepared by phosphate buffer solution (PBS, pH 7.4, 20 mM).

The synthetic oligonucleotides were obtained from Shenggong Bioengineering Co., Ltd (Shanghai, China) with the following sequences.

Hairpin DNA probe (pDNA): 5'-$H_2N$-$(CH_2)_3$-ACT AGA GTT CAA AAG CCC TTC AAC TCT AGT-$(CH_2)_6$-SH-3'; target DNA (tDNA): 5'-GAA GGG CTT TTG AAC TCT-3'; one-base mismatch, 5'-GAA GGG CTT TTG TAC TCT-3'; three-base mismatch, 5'-GAA CGG CTA TTG AAG TCT-3'; noncomplementary, 5'-CTC TCG CCA TGG CGT ACG-3'.

The sequences of two pairs of primers for PCR amplification of CML gene sample were designed according to the literature:[1,2] Primer 1: 5'-CGG GAG CAG CAG AAG AAG TGT-3', Primer 2: 5'-AAA GGT TGG GGT CAT TTT CAC-3', B-actin Primer 1: 5'-CAT CTC TTG CTC GAA GCT CA-3', B-actin Primer 2: 5'-ATC ATG TTT GAG ACC TTC AAC A-3'.

**Apparatus.** PEC measurements were performed on a Zahner PEC workstation (ZAHNER- elektrik GmbH & Co. KG, Germany) with a conventional three-electrode system: a platinum wire as counter electrode, a saturated Ag/AgCl electrode as reference electrode, and a modified ITO with an area of 0.5×0.5 $cm^2$ as working electrode. Field-emission scanning electron microscopy (FE-SEM) was carried out on a Hitachi S-4800 scanning electron microscope (Hitachi Co., Japan). High-resolution

transmission electron microscopy (HRTEM) was performed with a JEM-2100 transmission electron microscope with an accelerating voltage of 200 kV (Hitach, Japan). X-ray photoelectron spectroscopy (XPS) was performed using an ESCALAB 250Xi spectrometer (Thermo Fisher Scientific, UK) with a monochromatic Al Kα X-ray source, and all spectra were calibrated by normalizing the C (1s) peak to the standard value of 284.6 eV. UV–visible (UV–vis) absorption spectra were tested on a UV-3600 UV–visible spectrophotometer (Shimadzu, Japan). Photoluminescence (PL) spectra were recorded by an F-7000 fluorescence spectrometer (Hitach, Japan). UV–vis di□use reflectance spectra (UV–vis DRS) were recorded on a spectrophotometer (Hitachi U-3010, Japan) with fine $BaSO_4$ powder as reference. Confocal fluorescence imaging was performed on a confocal laser scanning microscope (LEICA TCS SP5, Germany).

**Synthesis of AuNPs.** The water-soluble AuNPs were synthesized by literature method with minor modifications.[3] Typically, 1.5 mL of 25 mM $HAuCl_4$ and 5 mL of 10 mM sodium citrate were mixed gradually in a round-bottomed flask under continuous stirring. Afterwards, 1.5 mL of 0.1 M ice-cold $NaBH_4$ was quickly injected into the solution above, and then it turned into orange-red color, indicating the particle formation. Thereafter, the mixed solution was stirring for another 6 h at room temperature with the color changing from orange-red to wine-red. Finally, the resulting AuNPs solution was obtained and stored at 4 °C prior to use.

**Synthesis of AuNPs-pDNA Conjugates.** Typically, 50 μL of 10 μM hairpin DNA probe (pDNA) was activated first by adding 5 μL of 10 μM TCEP for 1 h to break the disulfide bond between sulfhydryl functionalized pDNA. Then, 500 μL of purified AuNPs solution was added in the pDNA solution and incubated for 30 min under shaking. In order to prevent nonspecific adsorption of the AuNPs, 50 μL of 0.1 mM MCH was injected in the solution above and incubated for 2 h under shaking. After the resulting mixture was centrifuged for several times, the desired AuNPs-pDNA conjugates were acquired.

**Fabrication of NiO/ITO Electrode.** Before use, bare ITO slices were ultrasonically cleaned in order with acetone, 1 M NaOH of ethanol/water mixture (1:1, v/v) and DI water for 15 min, and then dried at 80 °C. NiO thin film was produced on the ITO substrate by hydrothermal method.[4] The reaction solution containing 0.25 M $C_6H_{12}N_4$ and 0.25 M $Ni(NO_3)_2$ was first transferred into a Teflon-lined digestion vessel, and then the ITO substrates were immersed oppositely into the reaction solution.

The closed digestion vessel was put in an oven and then heated at 90 °C for 10 min. After washed with DI water several times, the pre-treated ITO electrodes were annealed at 300 °C for 30 min in air and then cooled down to room temperature naturally to obtain the desired NiO/ITO electrode.

**Synthesis of CdTe QDs.** The water-soluble COOH-capped CdTe QDs were synthesized by modified means reported previously.[5] Typically, 0.6 mmol $CdCl_2 \cdot 2.5H_2O$ and 1.02 mmol MPA were mixed in a three-necked flask with constant stirring. Thereafter, the pH of the solution was adjusted to 11.8 by dropwise addition of 1.0 M NaOH and then the solution was bubbled with pure nitrogen gas for 30 min. Afterwards, 0.06 mmol $Na_2TeO_3$ and 120 mg $NaBH_4$ were successively added into the flask with the typical molar ratio of $Te^{2-}$: $Cd^{2+}$: MPA was 0.1/ 1/ 1.7. Finally, the desired CdTe QDs were obtained by heating at 100 °C and refluxing for 10 min under nitrogen gas protection.

**Fabrication of CdTe/NiO Photocathode.** The modification of CdTe QDs on the NiO/ITO electrode was according to a layer-by-layer assembly method via electrostatic adsorption. Specifically, the as-prepared NiO/ITO electrode was immersed successively into a positively charged 0.5 % (w.t.) PDDA solution containing 0.1 M NaCl for 10 min and a negatively charged CdTe QDs solution for another 20 min. In each immersing step, the electrode was washed with DI water. Afterwards, this process was again done three times for obtaining the desired CdTe/NiO photocathode.

**Preparation of Cathodic DNA Biosensor.** Typically, AuNPs-pDNA conjugates were immobilized on the CdTe/NiO photocathode via covalent bond between -COOH groups of the CdTe QDs and $-NH_2$ groups of the pDNA. Specifically, the CdTe/NiO photocathode was first incubated in the solution containing EDC (20 mM) and NHS (10 mM) for 30 min at room temperature and then washed with DI water. After that, 20 μL of AuNPs-pDNA conjugates solution was dropped on the activated CdTe/NiO photocathode and incubated at 4 °C humid atmosphere for 12 h, followed by rinsing with washing buffer solution (PBS, 20 mM, pH 7.4) to remove the unbound AuNPs-pDNA conjugates. The electrode was then blocked by adding 20 μL of 1 mM MEA for 1 h at room temperature. After rinsed with washing buffer solution, the resulting electrode was employed as a cathodic PEC biosensor and incubated with 20 μL of different concentrations of target DNA (tDNA) at 37 °C for 1 h. Finally, the electrode was rinsed with washing buffer solution and was ready for PEC detection.

**PEC Measurement.** PEC detection was carried out at room temperature in PBS (20 mM, pH 7.4). Oxygen ($O_2$) dissolved in the electrolyte was served as electron acceptor during the photocurrent test. A

LED lamp with a spectral of 430 nm was employed as the irradiation source with the light intensity of 350 W/$m^2$, which was switched on and off every 10 s. The involved electrochemical method was chopped light voltammetry, and the applied voltage was 0.0 V.

**Preparation of PCR products from real samples.** K562 cell and negative real sample (normal T lymphocyte) were supplied by the Eighth People's Hospital of Qingdao. Clinic cDNA template, which was obtained by reverse transcription from total RNA, was offered by the hospital. The PCR amplification procedure referred to the previous literature.[2] Briefly, polymerase chain reaction (PCR) was performed in a final volume of 50 μL containing 5.0 μL of clinic cDNA template, 1.0 μL of 10 μM each primer and 25 μL of Premix Taq (2×Taq buffer, 0.4 mM of dNTPS, 1.25 U of DNA polymerase). After an initial denaturation at 95 °C for 5 min, 34 cycles of PCR were conducted with denaturation at 94 °C for 30 s, annealing at 65 °C for 45 s and extension at 72 °C for 50 s, and then followed by a final extension at 72 °C for 6 min. The PCR products were denatured by heating at 95 °C for 10 min in a water bath, and then immediately chilled in an ice bath for 5 min to obtain single-stranded DNA for the next detection.

## Section 2: XPS Characterization of CdTe/NiO Photocathode

In order to study the valence states and chemical compositions of the CdTe/NiO photocathode, XPS was conducted. Fig. S1A presents full-scan XPS spectrum of the CdTe/NiO hybrid film, and the typical elements of Ni, C, O, Te and Cd were indicated. The high-resolution XPS spectra of C 1s, Ni 2p, C 1s, O 1s, Cd 3d, and Te 3d for the CdTe/NiO hybrid film were also depicted. The peak for C 1s at 284.6 eV in Fig. S1B served as the internal reference to correct the binding energy. The Ni 2p spectrum in Fig. S1C shows several peaks belonging to Ni $2p_{3/2}$ (peaks at 853.3, 855.2, and 860.4 eV) and Ni $2p_{1/2}$ (peaks at 871.8 and 879.1 eV). The O 1s spectrum in Fig. S1D displays two peaks located at 528.9 and 530.8 eV. The peaks at 528.9 eV was assigned to lattice oxygen in NiO crystal, while the peak at 530.8 eV can be ascribed to chemisorbed oxygen connected with NiO host.[6] As depicted in Fig. S1E of the Te 3d signal, the two prominent peaks of Te $3d_{5/2}$ at 572.0 eV and Te $3d_{3/2}$ at 582.5 eV could be observed, which could be assigned to tellurium elemental state (Cd−Te) from CdTe QDs.[7] Fig. S1F shows the Cd 3d spectrum with a Cd $3d_{5/2}$ peak at 404.7 eV and a Cd $3d_{3/2}$ peak at 411.5 eV. The XPS hence verified successful preparation of the CdTe/NiO hybrid film on the ITO electrode.

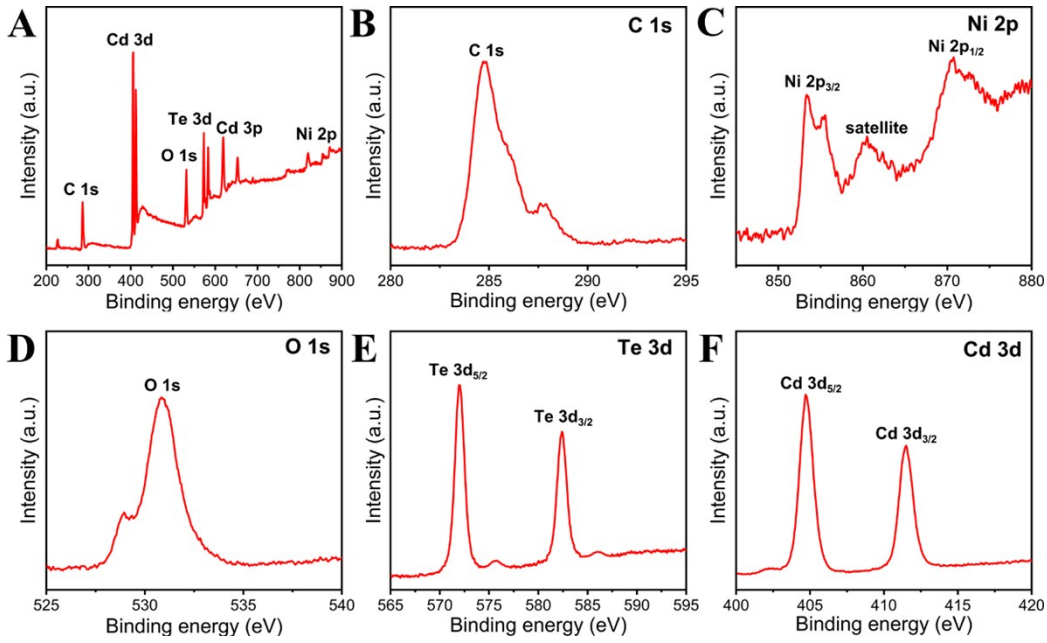


**Fig. S1.** (A) Full-scan XPS spectrum of the CdTe/NiO hybrid film; high-resolution XPS spectra of (B) C 1s, (C) Ni 2p, (D) O 1s, (E) Te 3d, and (F) Cd 3d for the CdTe/NiO hybrid film.

## Section 3: UV-vis DRS of CdTe/NiO photocathode

The light-absorption property of the CdTe/NiO photocathode was characterized by UV–visible diffuse reflectance spectroscopy (UV–vis DRS), as displayed in Fig. S2. The bare NiO nanofilm had little absorption from visible light owning to its large band gap excitation. After CdTe QDs modification, an evident absorption from visible light of the CdTe/NiO hybrid was clearly observed, which indicated the narrow band-gap of CdTe QDs and also verified sensitization action of the CdTe QDs to the 3D NiO nanofilm.

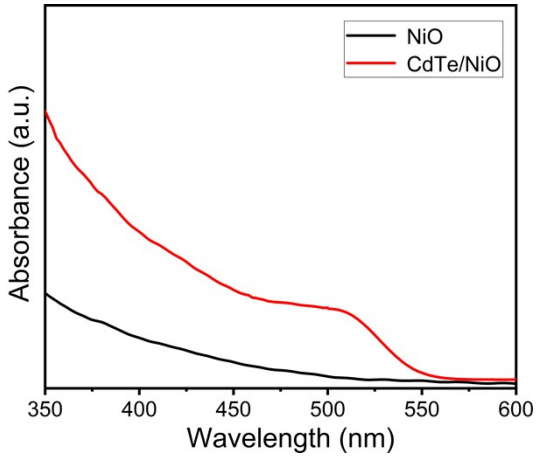


**Fig. S2**. UV-vis diffuse reflectance spectra of the NiO and CdTe/NiO modified ITO electrodes.

## Section 4: Characterization of AuNPs-pDNA Conjugates

The UV-vis absorption spectroscopy of the as-obtained AuNPs-pDNA conjugates is presented in Fig. S3. The pDNA had a sharp absorption peak at 260 nm (curve a), associating with the characteristic peak generated from the absorption of thymine and purine bases. The AuNPs showed an evident plasmon absorption peak at about 518 nm (curve b). After the conjugation between pDNA and AuNPs, the characteristic peak at 260 nm belonging to DNA sequence appeared in curve c, and meanwhile, the plasmon absorption peak of AuNPs red-shifted from 518 nm to 529 nm, which was because that the connection of pDNA on AuNPs via Au-S bond strengthened the trend of aggregation of AuNPs.[8] The UV-vis absorption spectra thus illustrated successful synthesis of the AuNPs-pDNA conjugates.

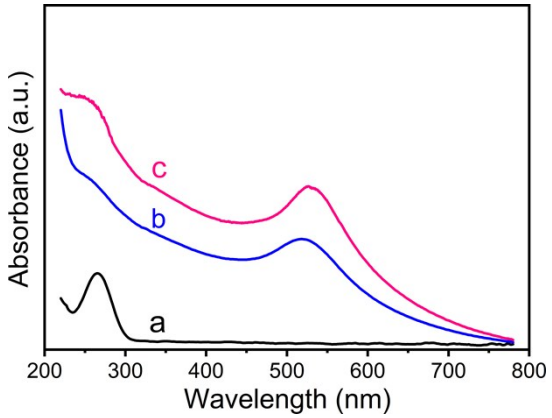


**Fig. S3**. UV-vis absorption spectra of the (a) pDNA, (b) AuNPs, and (c) AuNPs-pDNA conjugates.

## Section 5: Optical Imaging of the Sensing Electrode

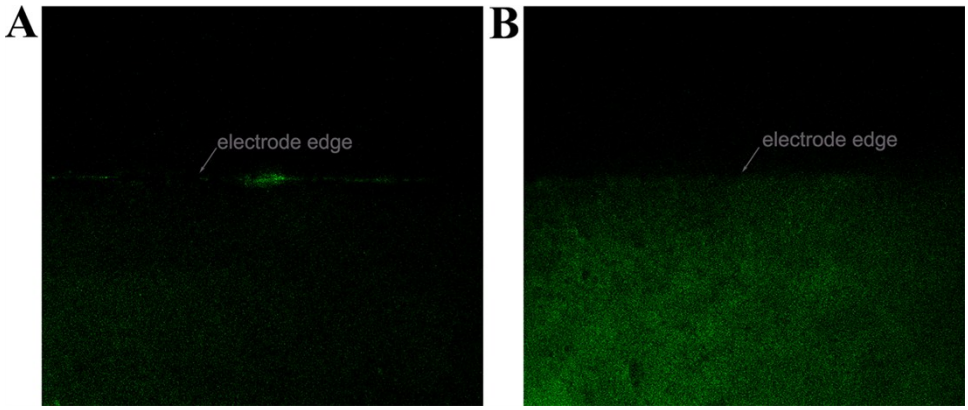


**Fig. S4.** Fluorescence images of the sensing electrode (A) before and (B) after tDNA hybridization.

## Section 6: Optimal condition of the biosensor

As the modification of CdTe QDs could influence the photocurrent of the CdTe/NiO photocathode evidently, the coating number of the CdTe QDs was optimized. Fig. S5 displays cathodic photocurrent of the CdTe/NiO photocathode obtained with different coating numbers of CdTe QDs. Along with increase of the coating number, the photocurrent of the CdTe/NiO photocathode gradually increased initially, and then it started to weaken after the coating number was beyond four. This variation trend can be explained that the increased coating number could supply plenty of the CdTe QDs to absorb the visible light at first, and then the excessive CdTe QDs would produce more and more surface recombination centers to block the charge transfer.[9] Thus, four coating number of the CdTe QDs was used to fabricate the CdTe/NiO photocathode.

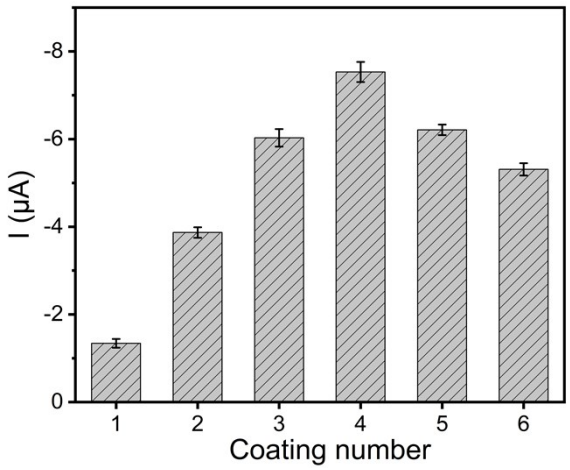


**Fig. S5.** Photocurrent responses of the CdTe/NiO photocathode obtained with different coating numbers of CdTe QDs.

## Section 7: Selectivity, stability, repeatability, and feasibility

The selectivity of the cathodic biosensor was inspected by introducing several different kinds of interfering species including diverse DNA sequences and some potential reductive reagents in the biological media. The DNA sequences involved were one-base mismatch, three-base mismatch and noncomplementary, while the potential reductive reagents were glutathione, glucose and ascorbic acid. As revealed in Fig. S6, an evident PEC signal to tDNA and minor or ignored PEC signals to those interfering species could be clearly observed. The comparing result verified that (i) the photocurrent signal was specifically triggered by the tDNA hybridization with pDNA and (ii) the elaborated DNA biosensor had a favorable anti-interference to potential reductive reagents.

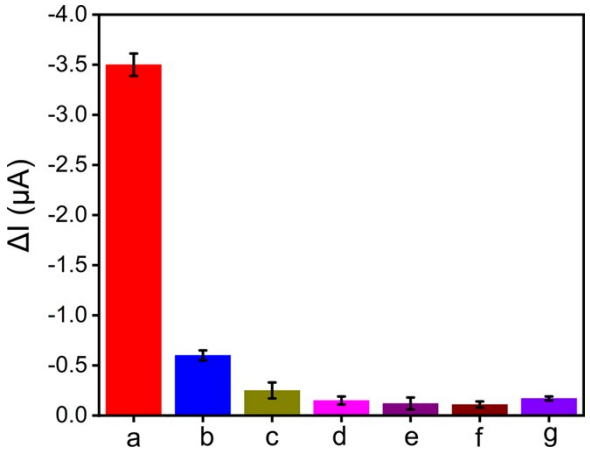


**Fig. S6.** Photocurrent signals of the cathodic PEC biosensor to 10 pM of tDNA, one-base mismatch, three-base mismatch and noncomplementary (a to d in order), and 1 mM of glutathione, glucose and ascorbic acid (e to g in order).

The stability of the cathodic biosensor was firstly appraised by time-varying photocurrent signal of the sensing electrode. As exhibited in Fig. S7, no obvious decay of the signal intensity was found after the sensing electrode encountered multiple periodic illuminations, verifying good PEC stability of the cathodic biosensor. In addition, the storage stability of the biosensor was also investigated. After the sensing electrodes were stored in a humid environment at 4 °C for ten days, the average signal intensity remained still 92.1% of the freshly prepared sensing electrodes, which pointed good long-term storage stability of the cathodic PEC biosensor.

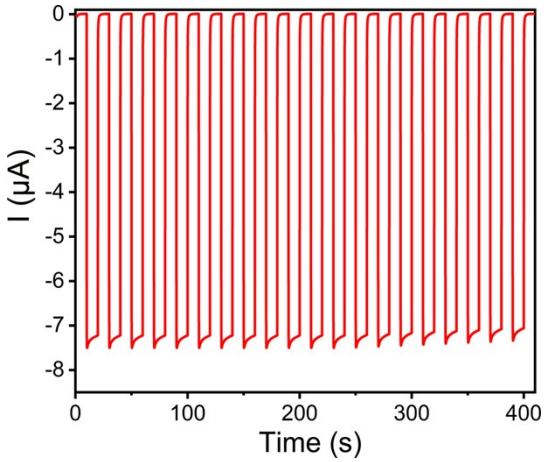


**Fig. S7.** Time-varying photocurrent signal of the cathodic sensing electrode.

The repeatability of the cathodic PEC biosensor was assessed by analyzing photocurrent signals of five independently fabricated sensing electrodes. The relative standard deviations (RSDs) of these

sensing electrodes against PEC detection of tDNA at the concentrations of 100 fM and 1 pM were 3.8% and 3.3%, which illustrated favorable reproducibility and accuracy of the biosensor.

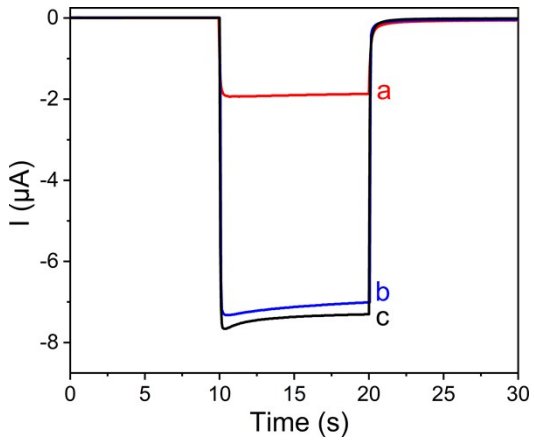


**Fig. S8.** Photocurrent responses of the cathodic PEC biosensor to PCR products of (a) K562 cell, (b) negative real sample, and (c) blank control.

The feasibility of the cathodic PEC biosensor was examined by detecting PCR products from K562 cell (positive cell strain) and negative real sample. As shown in Fig. S8, the photocurrent response of the cathodic PEC biosensor to the PCR products from K562 cell showed an evident decrease compared with the blank control (the probe signal), indicating that the DNA hybridization at electrode surface occurred. While for the negative real sample, the photocurrent response was nearly the same as the blank control, illustrating that the interaction between the negative real sample and the anchored probe DNA did not cause hybridization. The results above thus confirmed a promising application potential of the designed PEC biosensor.

## Section 8: References


1. A. H. Elmaagacli, D.W. Beelen, B. Opalka, S. Seeber, U.W. Schaefer. *Ann. Hematol.*, 2000, **79**, 424–431.
2. J. Chen, J. Zhang, K. Wang, X. Lin, L. Huang, G. Chen. *Anal. Chem.*, 2008, **80**, 8028–8034.
3. N. R. Jana, L. Gearheart, C. J. Murphy. *Langmuir*, 2001, **17**, 6782−6786.
4. L. Lepleux, B. Chavillon, Y. Pellegrin, E. Blart, L. Cario, S. Jobic, F. Odobel. *Inorg. Chem.*, 2009, **48**, 8245−8250.
5. G. C. Fan, L. Han, J. R. Zhang, J. J. Zhu. *Anal. Chem.*, 2014, **86**, 10877−10884.

6. J. L. Rodríguez, M. A. Valenzuela, T. Poznyak, L. Lartundo, I. Chairez. *J. Hazard. Mater.*, 2013, **262**, 472−481.
7. L. H. Jin, L. Shang, J. F. Zhai, J. Li, S. J. Dong. *J. Phys. Chem. C*, 2010, **114**, 803−807.
8. W. Haiss, N. T. K. Thanh, J. Aveyard, D. G. Fernig. *Anal. Chem.*, 2007, **79**, 4215−4221.
9. G. C. Fan, L. Han, H. Zhu, J. R. Zhang, J. J. Zhu. *Anal. Chem.*, 2014, **86**, 12398−12405.